NEOPLASIA
www.neoplasia.com

Volume 20 Number 12 December 2018 pp. 1187–1197 1187

Inducible Intestine-Specific Expression of *kras*^{V12} Triggers Intestinal Tumorigenesis In Transgenic Zebrafish[1]

Jeng-Wei Lu[2], Divya Raghuram[2], Pei-Shi Angelina Fong and Zhiyuan Gong

Department of Biological Sciences, National University of Singapore, Singapore

Abstract

KRAS mutations are a major risk factor in colorectal cancers. In particular, a point mutation of *KRAS* of amino acid 12, such as *KRAS* ^{V12}, renders it stable activity in oncogenesis. We found that *kras*^{V12} promotes intestinal carcinogenesis by generating a transgenic zebrafish line with inducible *kras*^{V12} expression in the intestine, *Tg*(*ifabp:EGFP-kras*^{V12}). The transgenic fish generated exhibited significant increases in the rates of intestinal epithelial outgrowth, proliferation, and cross talk in the active Ras signaling pathway involving in epithelial-mesenchymal transition (EMT). These results provide *in vivo* evidence of Ras pathway activation *via kras*^{V12} overexpression. Long-term transgenic expression of *kras*^{V12} resulted in enteritis, epithelial hyperplasia, and tubular adenoma in adult fish. This was accompanied by increased levels of the signaling proteins p-Erk and p-Akt and by downregulation of the EMT marker E-cadherin. Furthermore, we also observed a synergistic effect of *kras*^{V12} expression and dextran sodium sulfate treatment to enhance intestinal tumor in zebrafish. Our results demonstrate that *kras*^{V12} overexpression induces intestinal tumorigenesis in zebrafish, which mimics intestinal tumor formation in humans. Thus, our transgenic zebrafish may provide a valuable *in vivo* platform that can be used to investigate tumor initiation and anticancer drugs for gastrointestinal cancers.

Neoplasia (2018) 20, 1187–1197

Introduction

Colorectal cancer (CRC) accounts for 9% of global cancer incidence and is the fourth most common cause of cancer death [1]. The incidence rate is the highest in industrialized countries, such as in Europe and North America [1,2]. CRC generally occurs sporadically; however, hereditary factors can lead to the development of hereditary nonpolyposis colon cancer and familial adenomatous polyposis (Lynch et al., 2003), which account for 5% to 15% of all CRC cases. Heritable cases of CRC do not have a clearly defined mechanism and likely result from a combination of gene polymorphism, mutations in multiple susceptible loci, and environmental and dietary factors [3].

Numerous mutations have been shown to contribute to the development of CRC. For example, alterations in the Wnt/APC/β-catenin/TCF4 (T-cell factor-4) and TGF-β pathways have been frequently observed in CRC cases [4,5]. Mutations in RAF and phosphatidylinositol-3-kinase (PI3K) genes have also been found to increase cellular proliferation in CRC [4,6]. Single mutations in the tumor suppressor PTEN, which normally inhibits PI3K, have been shown to contribute to colorectal carcinogenesis [7]. Finally, mutations in the tumor suppressor TP53 have been observed in 40%-50% of CRC patients [8]. Mutations in TP53 are believed to be a late event in colorectal carcinogenesis and are thought to have a possible role in the transition from adenoma to carcinoma. The *KRAS* oncogene plays an important role in tumor initiation of CRC; indeed, *KRAS* mutations have been reported in approximately 30% of colorectal adenomas and in 30% to 50% of CRC patients [9].

Abbreviations: CRC, Colorectal cancer; DSS, dextran sodium sulphate; dpi, Days post-induction; EMT, Epithelial-mesenchymal transition; EGFP, Enhanced green fluorescent protein; FAP, Familial adenomatous polyposis; HNPCC, Hereditary nonpolyposis colon cancer; IACUC, Institutional Animal Care and Use Committee; mpf, month postfertilization; PFA, Paraformaldehyde; PI3K, phosphatidylinositol-3-Kinase; RT-qPCR, Quantitative reverse-transcription PCR; TCF4, T-cell factor-4; wpi, week post induction.

Address all correspondence to: Zhiyuan Gong, PhD, Department of Biological Sciences, National University of Singapore, Singapore. E-mail: dbsgzy@nus.edu.sg

[1] Competing Interests: None declared.

[2] These authors contributed equally.

Received 27 May 2018; Revised 10 October 2018; Accepted 11 October 2018

1476-5586
https://doi.org/10.1016/j.neo.2018.10.002

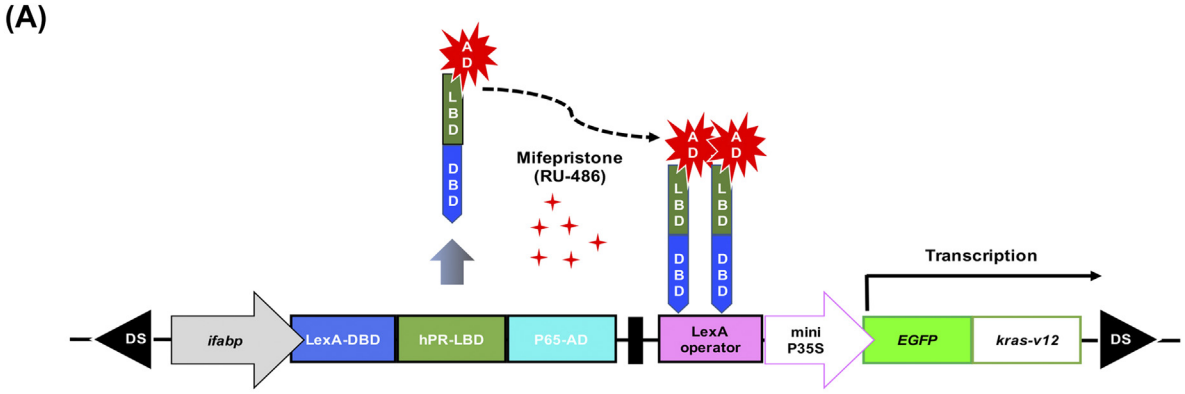
(A)
AD
LBD
DBD
Mifepristone
(RU-486)
Transcription
DS
ifabp
LexA-DBD
hPR-LBD
P65-AD
LexA
operator
mini
P35S
EGFP
kras-v12
DS

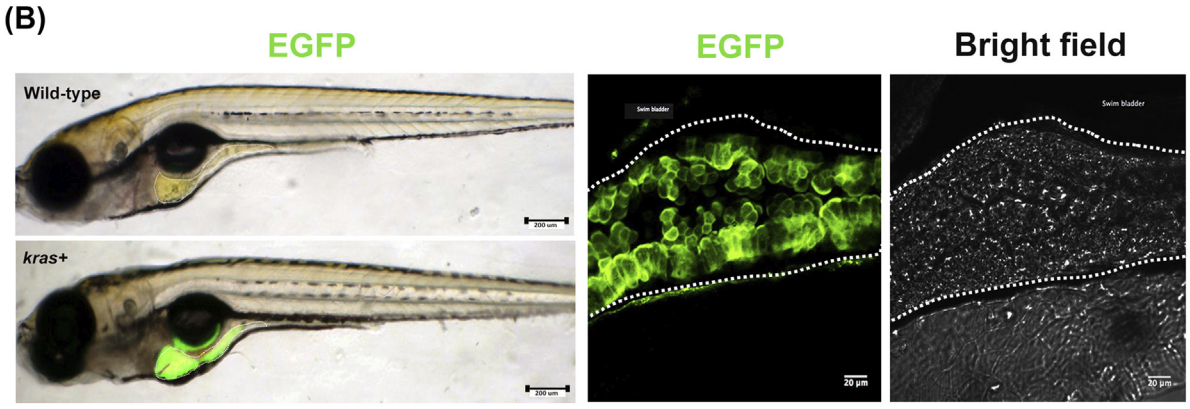
(B)
EGFP
EGFP
Bright field
Wild-type
kras+
Swim bladder
20 μm

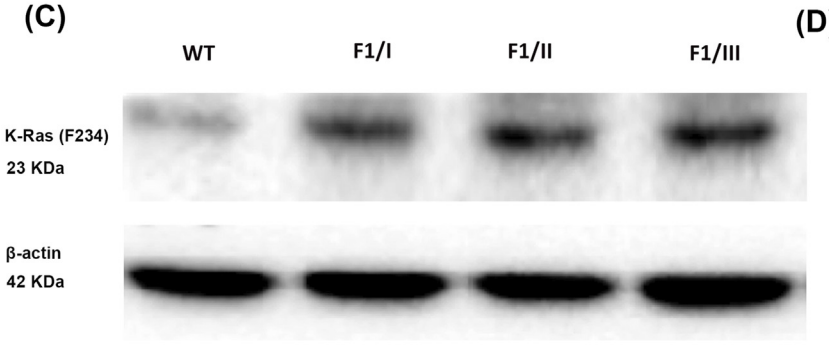
(C)
WT
F1/I
F1/II
F1/III
K-Ras (F234)
23 KDa
β-actin
42 KDa

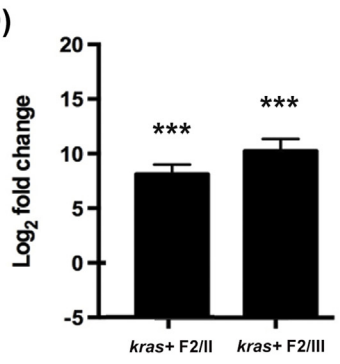
(D)
Log2 fold change
20
15
10
5
0
-5
***
***
kras+ F2/II
kras+ F2/III

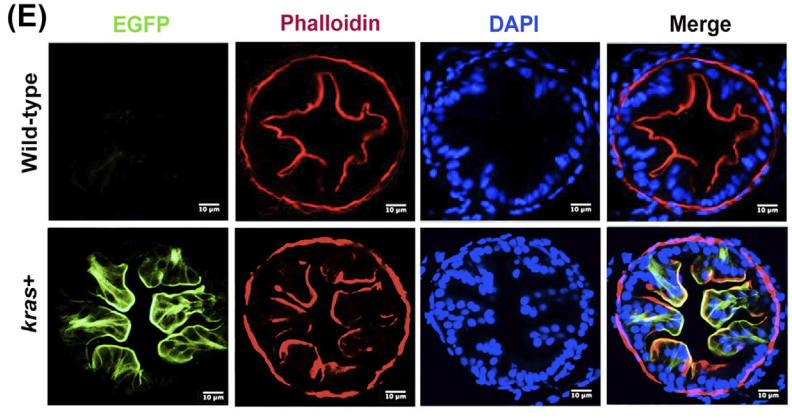
(E)
EGFP
Phalloidin
DAPI
Merge
Wild-type
kras+
10 μm

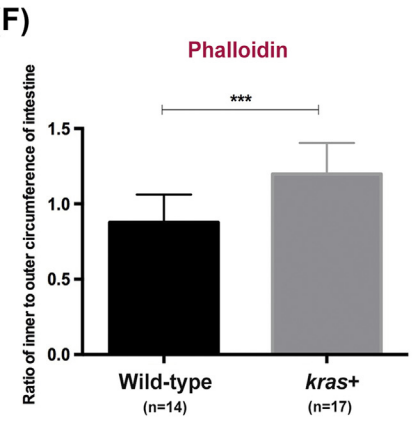
(F)
Phalloidin
***
Ratio of inner to outer circumference of intestine
1.5
1.0
0.5
0.0
Wild-type
(n=14)
kras+
(n=17)

Ras proteins are GTPases that are involved in intracellular signaling networks and play important roles in numerous cellular activities, including cell proliferation and differentiation. The *KRAS* gene encodes a 21-kDa GTPase that is transiently activated in response to extracellular stimuli or signals in the form of growth factors, cytokines, and/or hormones *via* cell surface receptors. Mutational activation of the *KRAS* gene reduces or abolishes intrinsic GTPase activity, thereby locking it in its GTP-bound conformation and leading to the constitutive activation of MAPK and PI3K/AKT signal transduction pathways [10]. This in turn results in the strong modulation of cell apoptosis, senescence, proliferation, motility, and differentiation [11–13].

The zebrafish model has several major advantages over other animal models, including easy and economical maintenance, high fecundity, and short generation time [14,15]. Several unique characteristics make the zebrafish model an ideal platform to study the molecular mechanisms which underlie human diseases, including intestinal disorders and tumors [15]. For example, the zebrafish is a vertebrate species and shares highly conserved anatomical structures and homologous organs with higher vertebrates including human. Furthermore, most of the signaling pathways which govern cell proliferation, apoptosis, differentiation, and movement are highly conserved between humans and zebrafish at the molecular level [16]. A high degree of homology and the presence of oncogenes and tumor suppressor genes suggest that oncogenic mechanisms are also highly conserved between zebrafish and higher vertebrates. Furthermore, zebrafish have been shown to spontaneously develop a wide variety of tumors with a histopathology that is comparable to those found in humans. Indeed, the low incidence of spontaneous tumor formation and sensitivity to many known human carcinogens suggest that zebrafish are a suitable model for the study of cancers relevant to humans [17]. Molecular analyses of carcinogens-induced zebrafish cancers also confirmed the high conservation of gene expression profile and signal pathways between zebrafish and human cancers [18,19].

In this study, we demonstrated that intestine-specific expression of *kras*^{V12} leads to the formation of intestinal tumors. We also showed that the overexpression of *kras*^{V12} triggers intestinal tumorigenesis *via* cross talk in the Ras pathway involved in epithelial-mesenchymal transition (EMT). Furthermore, *kras*^{V12} and DSS synergistically promoted intestinal tumors as indicated by histopathological examinations. Thus, our inducible Tg(*ifabp:kras*^{V12}) transgenic zebrafish model reported here could be used for the detailed analysis of intestinal tumor initiation, progression, and potential mechanisms for CRC.

Methods

Zebrafish Husbandry

Larvae and adult zebrafish (*Danio rerio*) were maintained using the established method described in our previous studies [20]. All experiments involving animals were approved by the Institutional Animal Care and Use Committee of the National University of Singapore (Protocol Number: 096/12). The aquarium was maintained with a photoperiod cycle of 14-hour light/10-hour dark.

Generation of Transgenic Zebrafish Using the Ac/Ds Transposon System

We sought to determine whether the expression of oncogenic *kras*^{V12} alters intestinal homeostasis by using the mifepristone-inducible LexPR system as previously described [21]. The DNA construct, pDs-*ifabp:LexPR-Lexop:EGFP-kras*^{V12}, possesses cDNA encoding a fusion protein consisting of enhanced green fluorescent protein gene (EGFP) at the N-terminal and zebrafish Kras^{V12} at the C-terminal. This fusion protein is under the control of the 4.5-kb intestine-specific *ifabp* promoter [21,22]. The construct also contains Ds transposon elements for facilitating chromosomal integration through the Ac transposase (Figure 1*A*) [23]. In brief, the pDs-*ifabp:LexPR-Lexop:EGFP-kras*^{V12} construct was created by replacing the *krt4* promoter of pDs-k*rt4:LPR-LOP:G4* [21] with the 4.5-kb *ifapb* promoter, and the *EGFP-kras*^{V12} genes were derived from the pDs-*fabp10:EGFP-kras*^{V12} plasmid [20]. To generate transgenic zebrafish, 10 pg of the above DNA construct and 50 pg *of* Ac transposase mRNA (synthesized *in vitro*) were co-injected into zebrafish embryos of one to two cells. The embryos were screened and reared to sexual maturity. The transgenic line was named Tg(pDs-*ifabp:LexPR-Lexop:EGFP-kras*^{V12}), which has been shortened to *kras*+ transgenic zebrafish in this paper.

RNA Extraction and Reverse Transcription PCR

Total RNA from intestinal tissue or zebrafish larvae (approximately 20 per treatment group) was isolated using TRIzol Reagent (Invitrogen). Three micrograms of RNA was then reverse-transcribed into cDNA using the Transcriptor First Strand cDNA Synthesis Kit in accordance with the manufacturer's instructions (Roche Applied Science). The cDNA samples were stored in a −80°C freezer before further processing.

Quantitative Reverse Transcription PCR

Quantitative reverse transcription PCR (RT-qPCR) was performed in a LightCycler 480 (Roche) with SYBR green as the detection dye (Power SYBR Green PCR Master Mix, Applied Biosystems). Genes of interest were amplified for up to 40 cycles of 95°C for 20 seconds, 65°C for 15 seconds, and 72°C for 30 seconds. All of the primers used in this study are listed in Supplementary Table 1.

Mifepristone Treatments of Zebrafish

Larvae were treated in six-well plates, and each treatment group included 20 larvae. Treatment involved the addition of 10 ml of E3 medium and 1 or 2 μM mifepristone (Sigma). Larvae were incubated

Figure 1. Generation and characterization of Tg(*ifabp:EGFP-kras*^{V12}) transgenic zebrafish. (A) Schematic diagram showing the DNA pDs-*ifabp:LexPR-Lexop:EGFP-kras*^{V12} construct used for the generation of *Tg(ifabp:EGFP-kras*^{V12}*)* transgenic fish. Ds, maize Ds transposon sequence. (B) Intestine-specific expression of EGFP-kras^{V12} in F1 transgenic fry and wild-type fish, and confocal image of whole mounted *kras*+ transgenic larva at 8 dpf following induction by 1 μM Mifepristone. The images were obtained at $z = 5$ μm over a thickness of 50 μm. (C) Western blot analysis of total proteins from WT and *kras*+ transgenic fish in the gut tissue from three founder lineage (I, II, and III) for the detection of the Kras protein. β-Actin, internal control for equal loading. (D) RT-qPCR analysis of *kras* RNA expression in the *kras* + transgenic F2 whole larvae from founders I and III. $N = 20$ larvae from each founder (at 2 dpi using 1 μM mifepristone) were used for isolation of proteins and mRNA. (E) Fluorescence micrographs of intestine cross sections from wild-type and *kras*+ zebrafish larvae showing green fluorescence or phalloidin staining. (F) Quantification of villi by ratio of inner to outer circumferences of intestine at 10 dpi by 2 μM mifepristone. Statistical significance: $^{***}P < .001$.

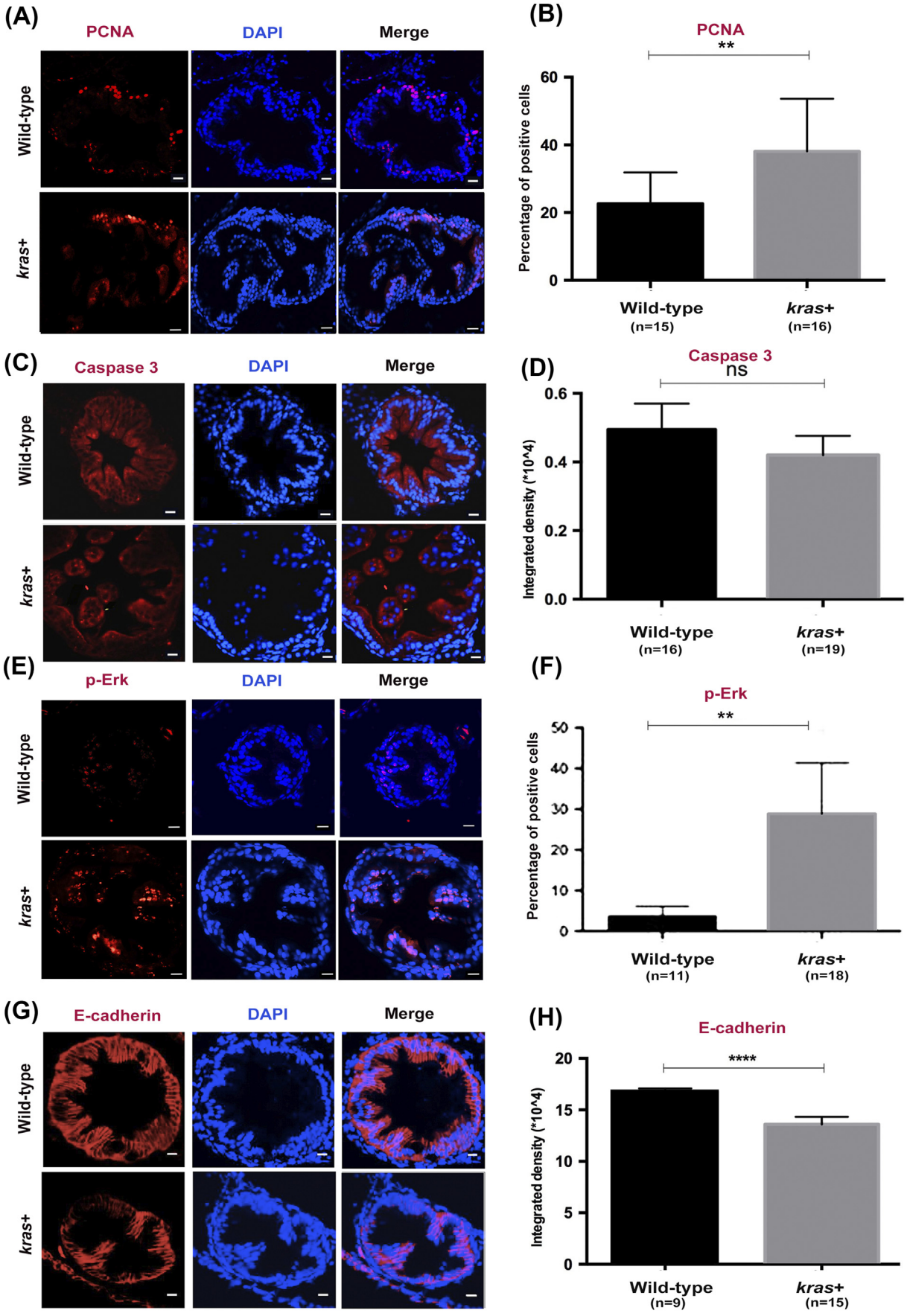
(A)
PCNA
DAPI
Merge
Wild-type
kras+
(B)
PCNA
**
Percentage of positive cells
60
40
20
0
Wild-type
(n=15)
kras+
(n=16)
(C)
Caspase 3
DAPI
Merge
Wild-type
kras+
(D)
Caspase 3
ns
Integrated density (*10^4)
0.6
0.4
0.2
0.0
Wild-type
(n=16)
kras+
(n=19)
(E)
p-Erk
DAPI
Merge
Wild-type
kras+
(F)
p-Erk
**
Percentage of positive cells
50
40
30
20
10
0
Wild-type
(n=11)
kras+
(n=18)
(G)
E-cadherin
DAPI
Merge
Wild-type
kras+
(H)
E-cadherin
****
Integrated density (*10^4)
20
15
10
5
0
Wild-type
(n=9)
kras+
(n=15)

at 28°C in an incubator, and mortality was determined daily. Water and fresh mifepristone were treated every other day. Adult fish were treated with 2 or 3 μM mifepristone in 5-l tanks. All tanks were kept in the dark at room temperature, and all adult fish were fed normally. Samples were collected at 2, 4, and 6 weeks postinduction (wpi) to investigate long-term induction effects.

Chemical Treatment of Zebrafish

For DSS treatment, *kras*+ transgenic fish and wild-type control fish were exposed with 0.0625% of DSS (Sigma) for 3 weeks. For induction of *kras*^{V12} expression from *kras*+ transgenic fish, 2 μM of mifepristone was used to induce 4–month postfertilization (mpf) fish for 3 weeks.

Histological and Cytological Analyses

Zebrafish were collected for histological analyses at different time points following mifepristone induction. Adult zebrafish (at indicated stages) were anesthetized using 0.02% tricaine (Sigma), whereupon various organs were collected and fixed in 10% neutral buffered formalin solution (Sigma) overnight. Larvae were fixed in 4% paraformaldehyde (Sigma) in PBS at 4°C and incubated in 60% 2-propanol for 10 minutes, after which the fixed tissues were embedded in paraffin, sectioned into 5-μm or 8-μm sections, and mounted on poly-L-lysine–coated slides. The slides were held in slide boxes at room temperature or −80°C. Zebrafish tissues were deparaffinized using Histo-Clear and rehydrated using serial dilutions of ethanol. Endogenous peroxidase activity was blocked by heating the slides for 10-15 minutes in antigen retrieval buffer (10 mM citric acid buffer, pH 6.0) and heated in a microwave oven at 100°C for 20 minutes. The slides were first cooled to room temperature and washed with three changes of 1× PBS. After blocking, primary antibodies were diluted overnight in a humidifying chamber (maintained at 4°C) using 5% BSA in 1× PBST. After being washed with 1× PBS, the slides were developed using the EnVision+ Dual Link System (Dako, Carpinteria, CA) and Substrate Chromogen System (Dako, Carpinteria, CA) or Alexa Fluor with conjugated secondary antibodies in accordance with the manufacturer's instructions. The online version of ImageJ software was used to quantify positively stained cells and the integrated density of cells. All antibodies used in this experiment are listed in Supplementary Table 1.

Histopathology of Zebrafish Intestines

Diagnoses of zebrafish intestinal histology were performed by a single-blind evaluation of all samples by hematoxylin and eosin (H&E) staining. For this, the *kras*+ transgenic fish intestine tissue was evaluated using four consecutive sagittal serial sections to cover the entire intestinal tract, anterior to posterior. Specifically, tissue samples were evaluated for epithelial hyperplasia, dysplasia, and the presence of neoplasia according to the diagnostic criteria previously described in [24].

Statistical Analyses

All statistical analyses for comparisons between experimental and control groups were performed using two-tailed Student's *t* tests and one-way analysis of variance (ANOVA). Kaplan-Meier estimation techniques were used to plot survival curves, and log-rank tests were used to examine differences between experimental and control groups [25]. *P* values of less than .05 were considered statistically significant.

Results

Generation of Tg(ifabp:EGFP-kras^{V12}*) Transgenic Zebrafish*

Zebrafish embryos were co-injected with synthetic Ac transposase mRNA at the one- to two-cell stage. To establish a stable transgenic line, F0 fish were crossed with wild-type fish, and their offsprings were screened for *EGFP* expression in the intestine. Three founder fish were identified to transmit the transgene to their progenies (F1). As shown in Figure 1*B*, 1 μM mifepristone induction resulted in *kras*^{V12} expression specifically in the intestinal tissue of the F1 progeny. Immunoblotting with anti–K-Ras-2B for Kras protein further confirmed that the expression of Kras protein was greatly increased in F1 fish from the three founders and had minimal staining of the endogenous Kras protein in wild-type control larvae (Figure 1*C*). RT-qPCR revealed that *kras*^{V12} was highly expressed in F2 whole larvae (Figure 1*D*), thereby confirming the results of immunoblotting analysis.

We subsequently characterized the sensitivity of the induction system using F2 larvae treated with different concentrations of mifepristone (0, 0.005, 0.05, 0.5, 2, and 4 μM) between 3 and 8 days postfertilization (dpf). We observed that *EGFP* was induced by various concentrations of mifepristone in the larval intestine in a dosage-dependent manner (Supplementary Figure 1, *A* and *B*). By RT-qPCR analyses, we found that transgenic *kras*^{v12} expression had no apparent effect on the expression of endogenous *kras* (data not shown).

To evaluate the effects of *kras*^{V12} expression in the intestine of larval zebrafish, we examined wild-type and *kras*+ transgenic fish at 10 days postinduction (dpi), which were induced with 2 μM mifepristone from 3 dpf. Most of the *kras*^{V12}-expressing larvae presented normal intestinal development with a histology similar to that of control wild-type larvae. However, phalloidin staining revealed a small but significant increase of intestinal folds in *kras*+ transgenic larvae, as measured by the ratio of inner to outer intestine circumference of *kras*+ larvae (Figure 1, *E* and *F*). Interestingly, *kras*^{V12} expression was mainly localized at the plasma membrane (Figure 1*E*), consistent with its active form as a membrane-associated GTP-bound protein. This is also similar to the expression of *EGFP-kras*^{V12} in the examination in our previously reported Tg(*lfabp:EGFP-kras*^{V12}) zebrafish, where we demonstrated that the transgenically expressed EGFP-Kras^{v12} was active and can be pulled down by RAS-RBD (Ras binding domain) [26]. Furthermore, activation of Kras downstream pathways such as p-Erk and p-Akt has also been demonstrated in previous studies [20,26–28].

Figure 2. *kras*^{V12} expression increases cell proliferation, Ras signaling, and EMT in the intestinal epithelium. Immunofluorescence staining (red) was carried out in intestine cross sections of wild-type and *kras*+ larvae at 8 dpf after 5 days of induction by 2 μM mifepristone. Only the intestine sections are shown. (A and B) Immunofluorescence staining of PCNA for cell proliferation (A) and quantification of percentage of positive cells (B). (C and D) Immunofluorescence staining of caspase 3 for apoptosis (C) and quantification of immunostaining density (D). (E and F) Immunofluorescence staining of p-Erk (E) and quantification of positive cells (F). (G and H) Immunofluorescence staining of E-cadherin (G) and quantification of immunostaining density (H). Immunostaining signals (D). Statistical significance: $^{**}P < .01$, $^{****}P < .0001$.

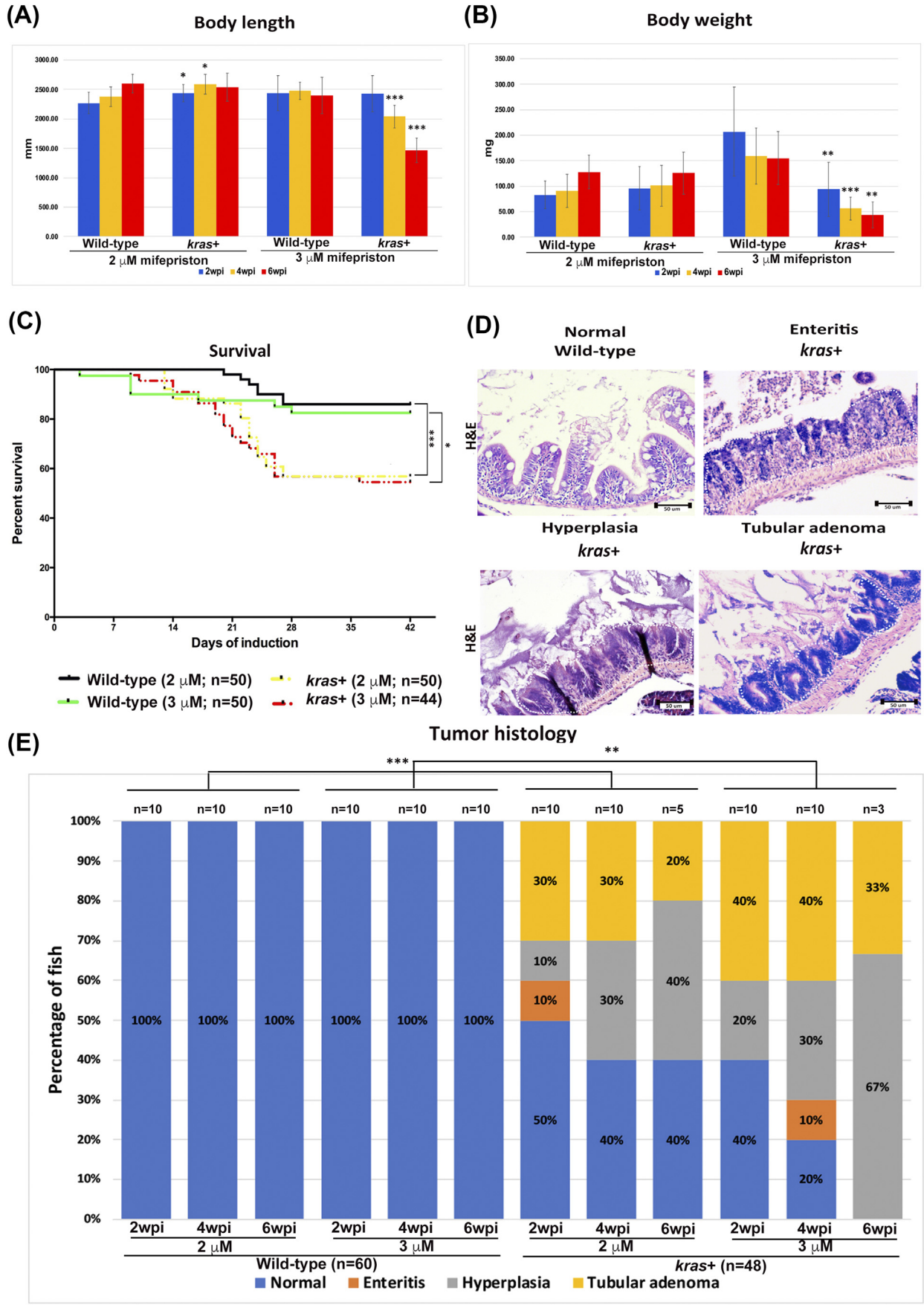
(A)
Body length
mm
Wild-type
kras+
2 μM mifepriston
3 μM mifepriston
2wpi 4wpi 6wpi
(B)
Body weight
mg
(C)
Survival
Percent survival
Days of induction
Wild-type (2 μM; n=50)
kras+ (2 μM; n=50)
Wild-type (3 μM; n=50)
kras+ (3 μM; n=44)
(D)
Normal
Wild-type
Enteritis
kras+
H&E
Hyperplasia
kras+
Tubular adenoma
kras+
(E)
Tumor histology
Percentage of fish
Wild-type (n=60)
kras+ (n=48)
Normal
Enteritis
Hyperplasia
Tubular adenoma

Effects of kras^{V12} *Expression on Cell Cycle and Levels of Phosphorylated Erk and E-Cadherin in Larval Zebrafish*

Next, we sought to elucidate the effects of *kras*^{V12} on the proliferation of intestinal cells. To determine the cell proliferation or apoptosis state of *kras*^{V12}-expressing intestines, we analyzed 8-dpf larval zebrafish that had been induced by 2 μM mifepristone for 5 days (Figure 2, *A* and *C*). We found that the overexpression of *kras*^{V12} led to a significant increase of PCNA-labeled cells, but not Caspase 3-labeled cells, in all 8-dpf *kras*+ transgenic larvae (Figure 2, *B* and *D*).

We previously demonstrated that expression of the *kras*^{V12} oncogene in the liver markedly stimulates Erk activity [26,27]. This led us to investigate whether *kras*^{V12} expression could also activate the Raf/Mek/Erk pathway in the intestine of zebrafish larvae. This pathway is a major downstream effector of Ras during intestinal cancer progression [29]. Immunofluorescence staining for phosphorylated Erk (p-Erk) demonstrated a dramatic increase of p-Erk in the intestine of *kras*+ compared to that of wild-type control fish (Figure 2, *E* and *F*). Furthermore, to examine the EMT state of *kras*^{V12}-expressing intestines, we also stained for E-cadherin and found that overexpression of *kras*^{V12} significantly decreased E-cadherin–labeled cells in *kras*+ transgenic larvae (Figure 2, *G* and *H*), implicating an increase of EMT activity.

Intestinal Tumor Phenotype In kras+ Transgenic Fish Caused by Sustained Expression of kras^{v12}

Heterozygous *kras*+ transgenic fish and wild-type control adult fish were used to further investigate the effect of sustained *kras*^{V12} expression on zebrafish intestinal tumorigenesis. Fish were administered with 2 μM and 3 μM mifepristone from 2 mpf. While the changes of body length in the 2 μM groups were not so obvious, *kras*+ fish in the 3-μM groups had significant reduction in body length at 4 and 6 wpi (Figure 3*A*). Similarly, induction with 3 μM mifepristone was also found to result in significantly lower body weight at 4 and 6 wpi (Figure 3*B*). Furthermore, some of the *kras*+ transgenic fish that had been induced with 2 or 3 μM mifepristone began dying at 9 dpi. By 6 wpi, most of the *kras*+ transgenic fish had died, whereas only a handful of the wild-type fish had died during the same period (Figure 3*C*).

Both *kras*+ and wild-type control fish were also examined by H&E staining. We evaluated the entire intestinal tract (anterior to posterior) of adult zebrafish for enteritis, epithelial hyperplasia, and the tumors at 2, 4, and 6 wpi (Figure 3*D*). We found that in all *kras*+ groups treated with either 2 μM or 3 μM mifepristone, hyperplasia and tubular adenoma in the intestine were commonly induced (Figure 3*E*). There was a general trend of dosage-dependent and time-dependent effects in the percentages and severity of induction of intestinal abnormalities. By 6 wpi, all *kras*+ fish in the 3 μM group were induced to either hyperplasia or tubular adenoma (Figure 3*E*). In addition, enteritis was also observed in a few *kras*+ fish in two groups (2 μM, 2 wpi; 3 μM, 4 wpi) (Figure 3*E*). In contrast, the wild-type control fish presented a normal pathology in all stages of both concentration groups. These results provide the first *in vivo* evidence that *kras*^{V12} overexpression in zebrafish facilitates intestinal carcinogenesis.

Increased Cell Proliferation and Phosphorylated Erk and Akt, and Downregulation of the EMT Marker E-Cadherin in Tubular Adenomas of kras+ Transgenic Fish

To elucidate the molecular mechanism in *kras*^{V12} transgenic adult fish, immunocytochemical stainings for PCNA, p-Erk, p-Akt, and E-cadherin were carried out. As expected, the PCNA+ proliferating cells were localized in the basal proliferation zone of intestinal villa in wild-type control fish, and PCNA was heavily stained throughout the tubular adenoma in *kras*+ fish (Figure 4, *A* and *B*). Similar to PCNA staining, heavy stainings for p-Erk and p-Akt were also observed in tubular adenoma in *kras*+ fish (Figure 4, *C-F*). In contrast, the expression of EMT marker E-cadherin appeared to be significantly downregulated in tubular adenoma of *kras*+ fish compared to that in the wild-type control fish (Figure 4, *G-H*). Consistent with our previous studies on fish larvae (Figure 2), these data revealed that the overexpression of *kras*^{V12} triggers cross talk along the Ras signaling pathway involved in EMT, and this may contribute to carcinogenesis in intestinal tissue.

Enhanced Intestinal Tumorigenesis in kras+ Transgenic Fish by DSS

It has been demonstrated that treatment of zebrafish larvae with the colitogenic agent DSS can induce intestinal inflammation with inflammatory bowel disease (IBD)–like characteristics [30]. To examine whether DSS could enhance tumorigenesis in the new *kras*+ transgenic zebrafish through induced inflammation, 4-mpf heterozygous *kras*+ were co-treated with 2 μM mifepristone and 0.0625% DSS for 3 weeks. We found that the body length of *kras*+ transgenic fish with DSS treatment was not significantly different from those of other control groups (Figure 5*A*). However, both DSS treatment and transgenic expression of *kras*^{V12} significantly reduced the body weight, and the reduction was compounded in *kras*+ fish with DSS treatment (Figure 5*B*).

Furthermore, some of the *kras*+ transgenic fish began dying at 7 dpi. By 3 wpi, 6 of the *kras*+ fish and 14 of the *kras*+*/DSS* fish died, whereas only 1 wild-type fish and 5 of *kras*+/DSS fish died during the same period (Figure 5*C*). We further evaluated the entire intestinal tract of adult zebrafish for enteritis, epithelial hyperplasia, and the presence of tumors at 3 wpi (Figure 5*D*). Intestinal samples were collected from *kras*+ (n = 20), *kras*+/DSS (n = 16), wild-type (n = 20), and wild-type/DSS (n = 20) groups for histological examination. While all wild-type fish showed normal intestinal histology, DSS treatment of wild-type fish caused enteritis in 5% fish and hyperplasia in 10% fish. Similar to the observation in earlier experiment shown in Figure 3, mifepristone-induced *kras*+ fish showed inflammation (10%), hyperplasia (30%), and tubular adenoma (35%). DSS treatment in *kras*+ fish further enhanced the abnormalities to 50% of fish for hyperplasia and 45% of fish for tubular adenoma (Figure 5*E*). These observations indicate that *kras*^{V12} expression and DSS synergistically caused intestinal tumor in transgenic zebrafish.

Figure 3. Phenotypic characterization of intestinal tumorigeneis in *kras*+ transgenic zebrafish. Wild-type and *kras*+ fish were treated with 2 or 3 μM mifepristone from 2 mpf, and samples were collected at 2, 4, and 6 wpi for gross observations and histological analyses. (A) Body length. (B) Body weight. (C) Survival curves. (D) Examples of normal, enteritis, hyperplasia, and tubular adenoma from H&E staining sections of intestine. Wild-type or *kras*+ fish sources of the sections are indicated. (E) Summary of intestinal histological abnormalities observed in wild-type and *kras*+ transgenic fish. The data were generated as a result of a blinded histological analysis. Numbers of fish in each group are indicated at the top of each bar. The differences among the variables were assessed using Student's *t* tests or one-way ANOVA. Statistical significance: *P < .05, **P < .01, ***P < .001.

Discussion

Human CRC is responsible for approximately 655,000 deaths every year [31]. In humans, the classical genetic events related to disease initiation and progression are the activation of mutations in the *KRAS* oncogene and the inactivation of mutations/deletions in *APC* and *TP53* tumor suppressor genes [32]. In the *KRAS* gene, most deleterious mutations occur at codons 12, 13, and 61. In human CRC, the presence of the *KRAS* mutations is associated with an increase in invasive stages and liver metastasis [33–35]. Lung metastases carrying the oncogenic *KRAS* mutation are common in CRC cases, indicating

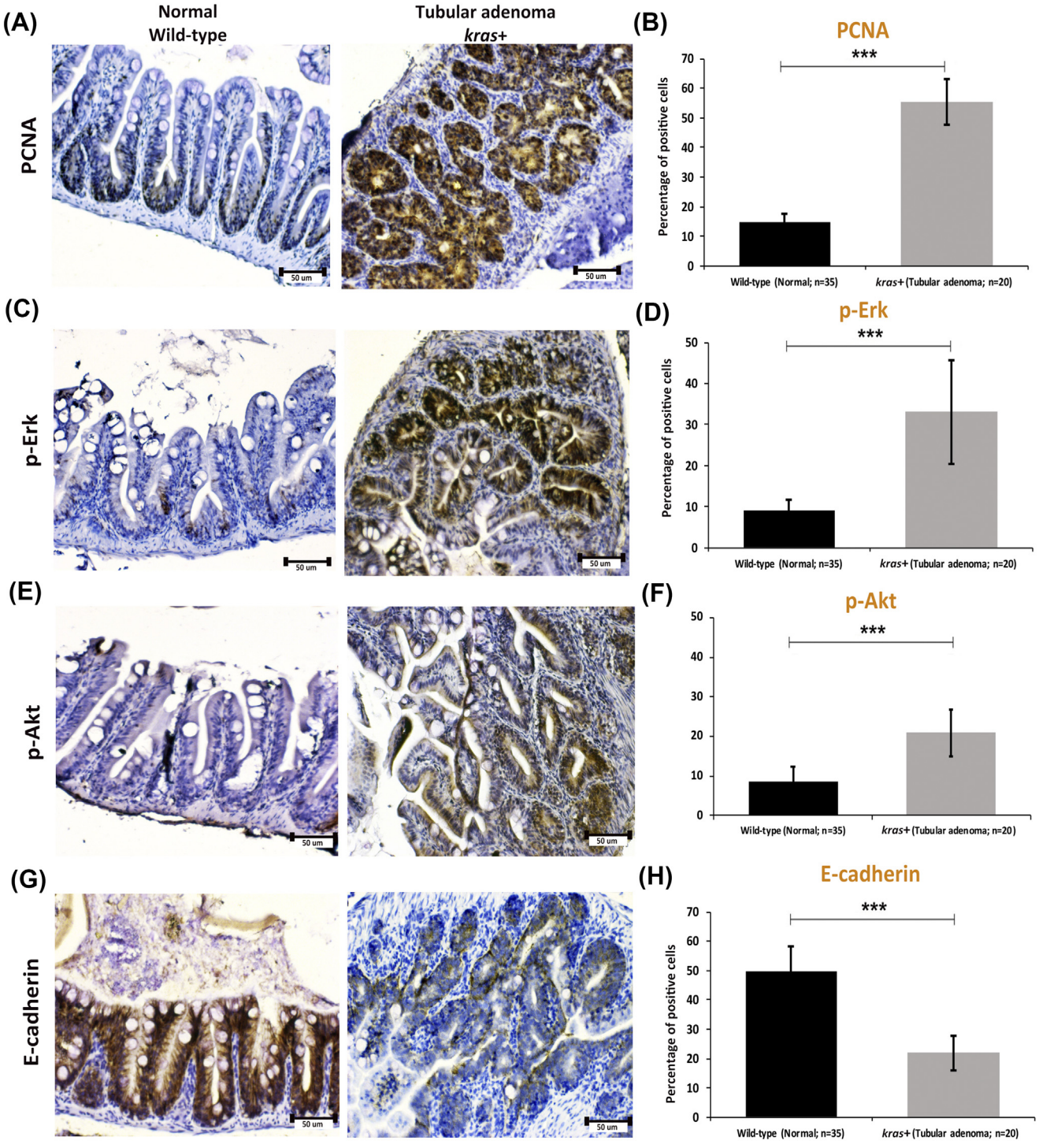

Figure 4. Immunocytochemical staining of PCNA, p-ErK, p-Akt, and E-cadherin in sections of normal intestine from wild-type fish and tubular adenoma from *kras*+ transgenic zebrafish. (A and B) Immunostaining of PCNA (A) and quantification of percentages of positive cells (B). (C and D) Immunostaining of p-Erk (C) and quantification of percentages of positive cells (D). (E and F) Immunostaining of p-Art (E) and quantification of percentages of positive cells (F). (G and H) Immunostaining of E-cadherin (G) and quantification of percentages of positive cells (H). Numbers of samples from each group are indicated in the quantification histograms. Statistical significance: ***$P < .001$.

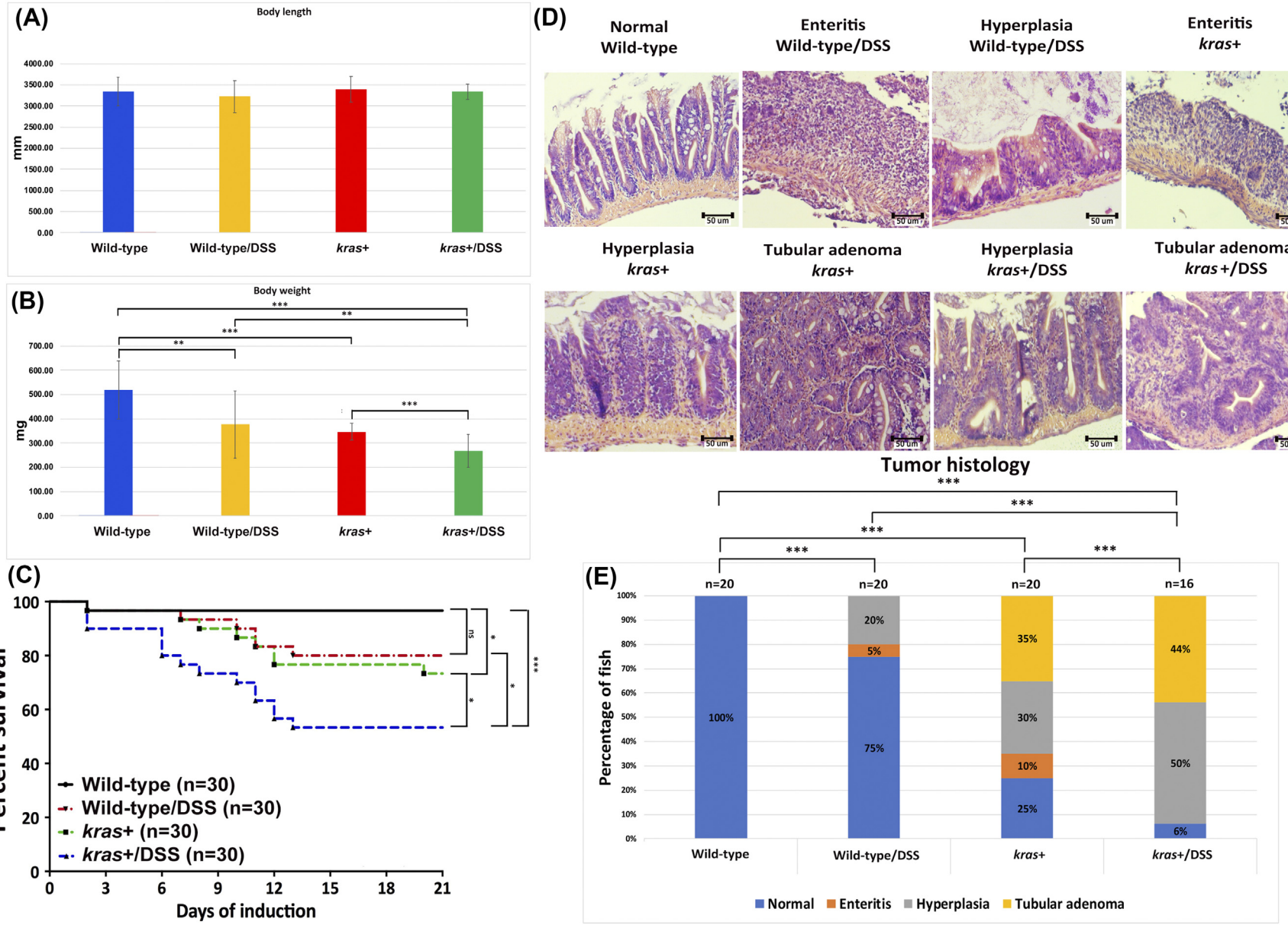

Figure 5. Synergistic effect of *kras*^{V12} expression and DSS on intestinal tumorigenesis. Four-mpf wild-type and *kras*+ fish were co-treated with 2 μM mifepristone and 0.0625% DSS for 3 weeks, and samples were collected for gross observations and histological analyses. There were four groups in the experiment: wild type, wild type/DSS, *kras*+, and *kras*+/DSS. (A) Body length. (B) Body weight. (C) Survival curves. (D) Examples of normal, enteritis, hyperplasia, and tubular adenoma from H&E staining sections of intestine. Sources of the sections are indicated. (E) Summary of intestinal histological abnormalities observed in the four experimental groups. The data were generated as a result of a blinded histological analysis (wild type, $n = 20$; wild type/DSS, $n = 20$; *kras*+, $n = 20$; *kras*+ with DSS, $n = 16$). The differences among the variables were assessed using Student's *t* tests or one-way ANOVA. Statistical significance: $^{*}P < .05$, $^{**}P < .01$, and $^{***}P < .001$.

that oncogenic *KRAS* plays an important role in tumor progression [36]. A number of therapeutic strategies targeting the *KRAS* signaling pathway have achieved limited clinical success. Several recent reports have also described the cooperative role of *RAS* isoforms in modulating drug sensitivity [37]. Metastasis of the primary colorectal tumor is directly related to patient survival; however, approximately 90% of all cancer deaths arise from the metastatic dissemination of primary tumors [38]. This underlines the importance of investigating carcinogenic effects in animal models and establishing an effective drug screening platform.

The zebrafish is an excellent model for *in vivo* investigation of disease mechanisms relevant to human disease including cancers and can also serve as a platform for the screening of therapeutic drugs [15,39]. Several previous studies in zebrafish cancer models in the brain [40], liver [20,26–28], and pancreas [41] have demonstrated that continued *kras*^{V12} expression is required for tumor maintenance. Tumors induced in zebrafish share many similar features with those in humans [20,40,41]. In this study, we established an effective intestinal tumor model that features inducible control of *kras*^{V12} expression in the intestine of transgenic fish. Specifically, induction is controlled *via* a mifepristone-inducible LexPR system [21]. The intestine-specific expression of *kras*^{V12} in zebrafish leads to enhanced cell proliferation (Figures 2, *A* and *B*; 4, *A* and *B*). This can in turn cause intestinal transformation such as epithelium outgrowth (Figure 1, *E* and *F*), enteritis, hyperplasia, and tubular adenoma (Figure 3*D*). In addition, *kras*^{V12} overexpression promotes Erk and Akt phosphorylation (Figures 2, *E* and *F*; 4, *C* and *D*; *E* and *F*) and leads to the downregulation of E-cadherin, a molecular marker signaling enhanced EMT (Figures 2, *G* and *H*; 4, *G* and *H*). The activation of these target genes may be mediated by the activation of the Ras signal pathway. The activation of ERK and AKT *via* phosphorylation allows this kinase to enter the cell nucleus and activate transcription factors, such as Jun and Fos [42,43], which are involved in cell proliferation [43,44]. Our data indicate that *kras*^{V12} and phosphorylation of Erk and Akt can be linked through cross talk on the Ras signal pathway involved in EMT. This may be a mechanism that underlies the development of intestinal carcinogenesis in *kras*+ transgenic fish.

In previous research on Lox-STOP-Lox mice, *Kras*^{V12} caused minor effects in the intestine, and this did not lead to tumor development [45]. Synergy between oncogenic factors in tumorigenesis has been reported in both mouse and zebrafish models. However, the *Kras*^{V12} point mutation was shown to accelerate intestinal carcinogenesis in *Apc* mutant mice [45] as well as in tumors induced by treatment with 1,2-dimethylhydrazine [46]. These results have shed light on the consequences of amino acid substitution and deletion mutations for *KRAS* between oncogenic factors that are present in clinical CRC. Previously, it has been reported that intestinal-specific expression of *CagA* in transgenic zebrafish caused intestinal hyperplasia, but overexpression of *CagA* in p53 mutant zebrafish also caused hyperplasia and further led to the occurrence of small cell carcinoma and adenocarcinoma [24].

It has been previously shown that inflammation such as IBD increases the risk of CRC [47–49]. Recently, DSS has been reported to induce inflammation of the colonic mucosa and have tumor-promoting effect in the mouse model [50]. Moreover, inflammation/inflammatory stimuli induced by treatment with 2% DSS after initiation with carcinogens is effective for rapid induction of colon tumors that possess *B-catenin* gene mutations [51,52]. *In-vivo,* the 2% [53] or 4% [54] DSS alone also caused the development of small intestinal polyp or tumor, suggesting a relationship between chronic inflammation and small intestinal tumorigenesis [55]. DSS-induced IBD-like enterocolitis has also been established in zebrafish [30] which is a tractable model of stress-induced mucus production [56].

In our present study, we established a new transgenic zebrafish model with inducible expression of oncogenic *kras*^{V12} specifically in the intestine and observed high rates of intestinal tumors (Figures 3*E* and 5*E*). We also found the collaborative effect of *kras*^{V12} and DSS for enhanced intestinal tumorigenesis in the new transgenic model. To the best of our knowledge, these results provide the first direct *in vivo* evidence for oncogenic *kras*^{V12} and provide a robust model of *kras*^{V12}-induced intestinal tumors in zebrafish. Furthermore, our mifepristone-inducible *kras*^{V12} transgenic fish provides an *in vivo* model for future investigation into *kras*^{V12}-induced intestinal carcinogenesis, in particular for tumor initiation.

Authors' Contributions

J. W. L., D. R., and Z. G. conceived the experiments and wrote the manuscript. J. W. L. and D. R. performed the experiments and analyzed data.

Acknowledgements

This work was supported by grants from Ministry of Education of Singapore (R154000667112 and R154000A23112).

Appendix A. Supplementary data

Supplementary data to this article can be found online at https://doi.org/10.1016/j.neo.2018.10.002.

References

[1] Haggar FA and Boushey RP (2009). Colorectal cancer epidemiology: incidence, mortality, survival, and risk factors. *Clin Colon Rectal Surg* **22**, 191–197.
[2] Boyle P and Langman JS (2000). ABC of colorectal cancer: epidemiology. *BMJ* **321**, 805–808.
[3] Jasperson KW, Tuohy TM, Neklason DW, and Burt RW (2010). Hereditary and familial colon cancer. *Gastroenterology* **138**, 2044–2058.
[4] Kinzler KW and Vogelstein B (1996). Lessons from hereditary colorectal cancer. *Cell* **87**, 159–170.
[5] Peignon G, Durand A, Cacheux W, Ayrault O, Terris B, Laurent-Puig P, Shroyer NF, Van Seuningen I, Honjo T, and Perret C, et al (2011). Complex interplay between beta-catenin signalling and Notch effectors in intestinal tumorigenesis. *Gut* **60**, 166–176.
[6] Grady WM and Carethers JM (2008). Genomic and epigenetic instability in colorectal cancer pathogenesis. *Gastroenterology* **135**, 1079–1099.
[7] Molinari F and Frattini M (2013). Functions and regulation of the PTEN gene in colorectal cancer. *Front Oncol* **3**, 326.
[8] Liu Y and Bodmer WF (2006). Analysis of P53 mutations and their expression in 56 colorectal cancer cell lines. *Proc Natl Acad Sci U S A* **103**, 976–981.
[9] Al-Kuraya KS (2009). KRAS and TP53 mutations in colorectal carcinoma. *Saudi J Gastroenterol* **15**, 217–219.
[10] Malumbres M and Barbacid M (2003). RAS oncogenes: the first 30 years. *Nat Rev Cancer* **3**, 459–465.
[11] Brooks DG, James RM, Patek CE, Williamson J, and Arends MJ (2001). Mutant K-ras enhances apoptosis in embryonic stem cells in combination with DNA damage and is associated with increased levels of p19(ARF). *Oncogene* **20**, 2144–2152.
[12] Plowman SJ, Berry RL, Bader SA, Luo F, Arends MJ, Harrison DJ, Hooper ML, and Patek CE (2006). K-ras 4A and 4B are co-expressed widely in human tissues, and their ratio is altered in sporadic colorectal cancer. *J Exp Clin Cancer Res* **25**, 259–267.
[13] Luo F, Brooks DG, Ye H, Hamoudi R, Poulogiannis G, Patek CE, Winton DJ, and Arends MJ (2007). Conditional expression of mutated K-ras accelerates intestinal tumorigenesis in Msh2-deficient mice. *Oncogene* **26**, 4415–4427.
[14] Lu JW, Hsieh MS, Liao HA, Yang YJ, Ho YJ, and Lin LI (2015). Zebrafish as a model for the study of human myeloid malignancies. *Biomed Res Int* **2015**, 641475.

[15] Lu JW, Ho YJ, Ciou SC, and Gong Z (2017). Innovative disease model: zebrafish as an in vivo platform for intestinal disorder and tumors. *Biomedicine* **5**.
[16] Liu S and Leach SD (2011). Zebrafish models for cancer. *Annu Rev Pathol* **6**, 71–93.
[17] Spitsbergen JM, Tsai HW, Reddy A, Miller T, Arbogast D, Hendricks JD, and Bailey GS (2000). Neoplasia in zebrafish (Danio rerio) treated with N-methyl-N'-nitro-N-nitrosoguanidine by three exposure routes at different developmental stages. *Toxicol Pathol* **28**, 716–725.
[18] Lam SH, Wu YL, Vega VB, Miller LD, Spitsbergen J, Tong Y, Zhan H, Govindarajan KR, Lee S, and Mathavan S, et al (2006). Conservation of gene expression signatures between zebrafish and human liver tumors and tumor progression. *Nat Biotechnol* **24**, 73–75.
[19] Xu H, Lam SH, Shen Y, and Gong Z (2013). Genome-wide identification of molecular pathways and biomarkers in response to arsenic exposure in zebrafish liver. *PLoS One* **8**e68737.
[20] Nguyen AT, Emelyanov A, Koh CH, Spitsbergen JM, Lam SH, Mathavan S, Parinov S, and Gong Z (2011). A high level of liver-specific expression of oncogenic Kras(V12) drives robust liver tumorigenesis in transgenic zebrafish. *Dis Model Mech* **4**, 801–813.
[21] Emelyanov A and Parinov S (2008). Mifepristone-inducible LexPR system to drive and control gene expression in transgenic zebrafish. *Dev Biol* **320**, 113–121.
[22] Her GM, Chiang CC, and Wu JL (2004). Zebrafish intestinal fatty acid binding protein (I-FABP) gene promoter drives gut-specific expression in stable transgenic fish. *Genesis* **38**, 26–31.
[23] Emelyanov A, Gao Y, Naqvi NI, and Parinov S (2006). Trans-kingdom transposition of the maize dissociation element. *Genetics* **174**, 1095–1104.
[24] Neal JT, Peterson TS, Kent ML, and Guillemin K (2013). H. pylori virulence factor CagA increases intestinal cell proliferation by Wnt pathway activation in a transgenic zebrafish model. *Dis Model Mech* **6**, 802–810.
[25] Lu JW, Hsieh MS, Hou HA, Chen CY, Tien HF, and Lin LI (2017). Overexpression of SOX4 correlates with poor prognosis of acute myeloid leukemia and is leukemogenic in zebrafish. *Blood Cancer J* **7**e593.
[26] Chew TW, Liu XJ, Liu L, Spitsbergen JM, Gong Z, and Low BC (2014). Crosstalk of Ras and Rho: activation of RhoA abates Kras-induced liver tumorigenesis in transgenic zebrafish models. *Oncogene* **33**, 2717–2727.
[27] Nguyen AT, Emelyanov A, Koh CH, Spitsbergen JM, Parinov S, and Gong Z (2012). An inducible kras(V12) transgenic zebrafish model for liver tumorigenesis and chemical drug screening. *Dis Model Mech* **5**, 63–72.
[28] Nguyen AT, Koh V, Spitsbergen JM, and Gong Z (2016). Development of a conditional liver tumor model by mifepristone-inducible Cre recombination to control oncogenic kras V12 expression in transgenic zebrafish. *Sci Rep* **6**19559.
[29] Fang JY and Richardson BC (2005). The MAPK signalling pathways and colorectal cancer. *Lancet Oncol* **6**, 322–327.
[30] Oehlers SH, Flores MV, Hall CJ, Okuda KS, Sison JO, Crosier KE, and Crosier PS (2013). Chemically induced intestinal damage models in zebrafish larvae. *Zebrafish* **10**, 184–193.
[31] Siegel RL, Miller KD, and Jemal A (2016). Cancer statistics, 2016. *CA Cancer J Clin* **66**, 7–30.
[32] Wood LD, Parsons DW, Jones S, Lin J, Sjoblom T, Leary RJ, Shen D, Boca SM, Barber T, and Ptak J, et al (2007). The genomic landscapes of human breast and colorectal cancers. *Science* **318**, 1108–1113.
[33] Li HT, Lu YY, An YX, Wang X, and Zhao QC (2011). KRAS, BRAF and PIK3CA mutations in human colorectal cancer: relationship with metastatic colorectal cancer. *Oncol Rep* **25**, 1691–1697.
[34] Modest DP, Stintzing S, Laubender RP, Neumann J, Jung A, Giessen C, Haas M, Aubele P, Schulz C, and Boeck S, et al (2011). Clinical characterization of patients with metastatic colorectal cancer depending on the KRAS status. *Anticancer Drugs* **22**, 913–918.
[35] Mannan A and Hahn-Stromberg V (2012). K-ras mutations are correlated to lymph node metastasis and tumor stage, but not to the growth pattern of colon carcinoma. *APMIS* **120**, 459–468.
[36] Pereira AA, Rego JF, Morris V, Overman MJ, Eng C, Garrett CR, Boutin AT, Ferrarotto R, Lee M, and Jiang ZQ, et al (2015). Association between KRAS mutation and lung metastasis in advanced colorectal cancer. *Br J Cancer* **112**, 424–428.
[37] Nandan MO and Yang VW (2011). An update on the biology of RAS/RAF mutations in colorectal cancer. *Curr Colorectal Cancer Rep* **7**, 113–120.
[38] Stein U and Schlag PM (2007). Clinical, biological, and molecular aspects of metastasis in colorectal cancer. *Recent Results Cancer Res* **176**, 61–80.
[39] Kirchberger S, Sturtzel C, Pascoal S, and Distel M (2017). Quo natas, Danio? Recent progress in modeling cancer in zebrafish. *Front Oncol* **7**, 186.
[40] Ju B, Chen W, Orr BA, Spitsbergen JM, Jia S, Eden CJ, Henson HE, and Taylor MR (2015). Oncogenic KRAS promotes malignant brain tumors in zebrafish. *Mol Cancer* **14**, 18.
[41] Provost E, Bailey JM, Aldrugh S, Liu S, Iacobuzio-Donahue C, and Leach SD (2014). The tumor suppressor rpl36 restrains KRAS(G12V)-induced pancreatic cancer. *Zebrafish* **11**, 551–559.
[42] Cisternas R (1975). Some physiological aspects of cholesterol metabolism (author's transl). *Rev Med Chil* **103**, 30–37.
[43] Zenonos K and Kyprianou K (2013). RAS signaling pathways, mutations and their role in colorectal cancer. *World J Gastrointest Oncol* **5**, 97–101.
[44] Ubeda M, Vallejo M, and Habener JF (1999). CHOP enhancement of gene transcription by interactions with Jun/Fos AP-1 complex proteins. *Mol Cell Biol* **19**, 7589–7599.
[45] Luo F, Brooks DG, Ye H, Hamoudi R, Poulogiannis G, Patek CE, Winton DJ, and Arends MJ (2009). Mutated K-ras(Asp12) promotes tumourigenesis in Apc (Min) mice more in the large than the small intestines, with synergistic effects between K-ras and Wnt pathways. *Int J Exp Pathol* **90**, 558–574.
[46] Luo F, Poulogiannis G, Ye H, Hamoudi R, Zhang W, Dong G, and Arends MJ (2011). Mutant K-ras promotes carcinogen-induced murine colorectal tumourigenesis, but does not alter tumour chromosome stability. *J Pathol* **223**, 390–399.
[47] Munkholm P (2003). Review article: the incidence and prevalence of colorectal cancer in inflammatory bowel disease. *Aliment Pharmacol Ther* **18**(Suppl. 2), 1–5.
[48] van der Woude CJ, Kleibeuker JH, Jansen PL, and Moshage H (2004). Chronic inflammation, apoptosis and (pre-)malignant lesions in the gastro-intestinal tract. *Apoptosis* **9**, 123–130.
[49] Seril DN, Liao J, Yang GY, and Yang CS (2003). Oxidative stress and ulcerative colitis-associated carcinogenesis: studies in humans and animal models. *Carcinogenesis* **24**, 353–362.
[50] Okayasu I, Hatakeyama S, Yamada M, Ohkusa T, Inagaki Y, and Nakaya R (1990). A novel method in the induction of reliable experimental acute and chronic ulcerative colitis in mice. *Gastroenterology* **98**, 694–702.
[51] Kohno H, Suzuki R, Sugie S, and Tanaka T (2005). Beta-Catenin mutations in a mouse model of inflammation-related colon carcinogenesis induced by 1,2-dimethylhydrazine and dextran sodium sulfate. *Cancer Sci* **96**, 69–76.
[52] Tanaka T, Suzuki R, Kohno H, Sugie S, Takahashi M, and Wakabayashi K (2005). Colonic adenocarcinomas rapidly induced by the combined treatment with 2-amino-1-methyl-6-phenylimidazo[4,5-b]pyridine and dextran sodium sulfate in male ICR mice possess beta-catenin gene mutations and increases immunoreactivity for beta-catenin, cyclooxygenase-2 and inducible nitric oxide synthase. *Carcinogenesis* **26**, 229–238.
[53] Tanaka T, Kohno H, Suzuki R, Hata K, Sugie S, Niho N, Sakano K, Takahashi M, and Wakabayashi K (2006). Dextran sodium sulfate strongly promotes colorectal carcinogenesis in Apc(Min/+) mice: inflammatory stimuli by dextran sodium sulfate results in development of multiple colonic neoplasms. *Int J Cancer* **118**, 25–34.
[54] Cooper HS, Everley L, Chang WC, Pfeiffer G, Lee B, Murthy S, and Clapper ML (2001). The role of mutant Apc in the development of dysplasia and cancer in the mouse model of dextran sulfate sodium-induced colitis. *Gastroenterology* **121**, 1407–1416.
[55] Barbour KW, Davis T, White A, Baumann H, and Berger FG (2001). Haptoglobin, inflammation, and tumorigenesis in the MIN mouse. *Redox Rep* **6**, 366–368.
[56] Oehlers SH, Flores MV, Hall CJ, Crosier KE, and Crosier PS (2012). Retinoic acid suppresses intestinal mucus production and exacerbates experimental enterocolitis. *Dis Model Mech* **5**, 457–467.